CONTROL DESIGN FRAMEWORK FOR AUTOMATED LANDING OF A VTOL DRONE ON A NAVAL SHIP DECK IN ADVERSE WEATHER

Tijmen Pollack, Ole Pfeifle, Stefan van ‘t Hoff, George Tzanetos Alevras, and Jan-Willem van Doorn,
Royal NLR - Netherlands Aerospace Centre, Amsterdam, The Netherlands

Mark Voskuijl, Netherlands Defence Academy (NLDA), Den Helder, The Netherlands

Eelco Frickel, Maritime Research Institute Netherlands (MARIN), Wageningen, The Netherlands

Abstract

This paper presents a design framework for automated landing of a lift-plus-cruise vertical take-off and landing (VTOL) unmanned aerial system on a naval ship deck in adverse weather conditions. The work is carried out as part of a project funded by the Dutch Ministry of Defense and has the goal of testing and extending operating limits of VTOL configurations on a naval vessel. The presence of strong relative winds and turbulence on a sailing vessel implies that a lift-plus-cruise configuration will commonly find itself in the transition regime during relative position-keeping and landing in this environment. This leads to a number of distinct challenges for control law design, which requires optimal use of the available control authority and bandwidth throughout the entire velocity regime. The proposed approach aims to extend the operating limits by applying robust control synthesis techniques to i) an existing, cascaded PID setup as benchmark and ii) a unified control law architecture based on incremental nonlinear dynamic inversion. A landing trajectory generation module based on predictions of the ship motion completes the automated landing system. The insights from this paper serve as a basis for control design and future real-world flight tests on a naval ship deck.

1. NOTATION

Acronyms:

CETI	Control Equivalent Turbulence Input
DGPS	Differential Global Positioning System
DRB	Disturbance Rejection Bandwidth
DRP	Disturbance Rejection Peak
HITL	Hardware-In-The-Loop
INDI	Incremental Nonlinear Dynamic Inversion
LOES	Low-Order Equivalent System
MBD	Model-Based Development
PID	Proportional-Integral-Derivative
SITL	Software-In-The-Loop
SUOL	Ship-UAS Operational Limits
UAS	Unmanned Aerial System
VTOL	Vertical Take-Off and Landing

2. INTRODUCTION

Small and medium-sized drones are increasingly used for various applications in the security and military domain. Within naval operations, their low cost and high degree of automation can provide valuable new capabilities. However, naval ship decks represent a challenging environment for both manned and unmanned aircraft with strong winds, gusts and turbulence in the ship’s air wake as well as the motion of the deck itself, while sailing at significant speeds. This paper describes the work carried out as part of a project funded by the Dutch Ministry of Defense on technology development for automated landings of UAS on naval ship decks under adverse weather conditions. The proposed

Figure 1: VTOL UAS test platform: DeltaQuad EVO

technology consists of (i) advanced control laws for gust and turbulence rejection in harsh ship wind climates and (ii) automated trajectory planning based on ship motion prediction. The UAS on which these technology developments are demonstrated is shown in Figure 1 and represents a lift-plus-cruise configuration. This configuration typically offers desirable mission capabilities by combining vertical take-off and landing (VTOL) with efficient wing-borne flight for increased range and endurance. The airframe has a maximum take-off weight of 10kg and cruise speed of 16.7m/s. Its four hover propellers allow it to take off and land vertically, whereas its wing, elevons and pusher propeller allow for efficient wing borne cruise flight.

Despite their advantages, however, the presence of aerodynamic surfaces leads to challenges in strong winds and gusts, as these lead to significant aerodynamic forces and moments. Furthermore, the particular mission profile of landing on a moving ship in non-zero winds implies that the UAS will commonly operate in the transition regime. Since good trajectory-following performance and desirable flying characteristics should be achieved in the critical phases of approach and landing, this means that significant performance and robustness is expected from the control laws. However, classical transition schemes typically blend or switch between hover and wing-borne flight controllers as a function of measured airspeed. This typically includes distinct front- and back-transition modes, during which the vehicle accelerates or decelerates (i.e., transitions) to or from stable wing-borne flight. The default control laws of the demonstrator UAS, which makes use of the PX4 Autopilot[2] system architecture, are also based on this strategy. However, in harsh maritime

Figure 2: Naval vessel used in the project: LPD-2. Credits: Mediacentrum Defensie

environments that are dominated by turbulence and gusts, the concept of front- or back-transition becomes void as the UAS is expected to perform station-keeping with respect to a moving reference while being subject to rapid changes in relative airspeed. Therefore, a blending or switching strategy is expected to lead to (severe) performance and handling issues and may (in some cases) even lead to instability. Moreover, in addition to challenges resulting from strong winds and flying in transition mode for prolonged times, the motion of a ship deck generally requires precise relative navigation and timing to avoid high relative vertical velocities and excessive relative bank angles at touch-down.

The project goal is to test and extend the operating limits of the demonstrator lift-plus-cruise configuration (Figure 1) for naval ship deck operation by (i) generation of landing trajectories that take into account the motion of the ship to minimize relative velocity at touch down and (ii) development of control laws and -logic that improve disturbance rejection and overall flying characteristics in strong turbulence and gusts. Besides the UAS and naval vessel used in this project (Figure 1 and Figure 2), the approach should be suitable for a larger range of Class 1, 2 UAS and different ships such that it can be applied to the future heterogenous drone fleet operated by the Netherlands Royal Navy.

With respect to landing trajectory generation, existing approaches can be divided into using a fixed trajectory in space and time (Refs. 1,2) or using trajectories optimized with respect to either the ship motion (Refs. 3,4) or the air wake (Refs. 5,6). The approach presented in this paper uses a trajectory that consists of a fixed vertical velocity profile and optimized touch-down timing based on motion predictions (Refs. 7,8). In terms of improved turbulence and gust rejection properties of UAS, existing litera-

[2]PX4 user guide: https://docs.px4.io/main/en/ (Retrieved July 25, 2025)

ture proposes a variety of different methods, ranging from gain tuning to maximize attenuation in relevant frequency bands (Refs. 9,10), adaptive control (Ref. 12), sliding-mode control (Ref. 13) and incremental control (Refs. 14-16). Within this project, two approaches are followed in parallel. First, a benchmark (i.e., standard) approach is followed to optimize the feedback gains for improved disturbance rejection of a cascaded Proportional-Integral-Derivative (PID) controller architecture with classical transition logic. This strategy requires relatively little modification to the default UAS control laws and connects naturally to the notable class of explicit model-following controllers (Refs. 9,17) when command models are incorporated as an additional feedforward degree-of-freedom; however, for the reasons listed before, it is anticipated to provide only small improvements for the operational limits. Therefore, a second, *unified* controller is proposed based on the principle of incremental nonlinear dynamic inversion (INDI) and extended control allocation techniques. This setup has been repeatedly shown in the literature to result in good performance over wide flight envelopes for (predominantly land-based) VTOL vehicles (see, e.g., Refs. 18-21). However, maritime applications of INDI-based control laws for UAS have been relatively scarce, with Ref. 22 forming a notable exception. For both the PID and INDI controller configurations, control design and analysis is performed based on model-based development (MBD) using a multidisciplinary simulation environment. The robust control framework forms the basis for systematic tuning of the available design parameters against a comprehensive set of requirements.

The presented benchmark and unified approaches will ultimately be tested in real-world flight tests to evaluate their potential for improving the ship-UAS operational limits (SUOLs) of the demonstrator lift-plus-cruise configuration for landing on a ship deck. It must be remarked that the project is agnostic of the positioning system used for relative navigation. For the demonstration flight tests, relative navigation will be provided by differential GPS with respect to the ship deck. The controller design will aim to achieve robustness to measurement error, time delays, data gaps, etc. representative for both DGPS and, e.g., optical means of relative positioning. With the latter, future scenarios such as ship deck landing in GPS-denied environments are anticipated for.

Summarizing, the contribution of this paper reads as follows: a robust, unified, incremental control framework is described for automated landing of a lift-plus-cruise UAS on a naval ship deck, including trajectory planning based on ship motion prediction and control laws for improved gust and turbulence rejection throughout the entire velocity regime, with the goal of testing and extending operating limits of such a configuration.

3. SIMULATION ENVIRONMENT OVERVIEW

Successful and efficient deployment of the automated landing system calls for a development process that is systematic and transparent in terms of design, verification, and validation. An MBD approach provides the necessary tools and capabilities to trace down specific functionalities and requirements to distinct system features. To this end, a nonlinear simulation environment is built that captures the relevant environmental and platform-specific behaviors for the required ship-deck landing conditions with a fidelity suitable for (early) control law development purposes. This involves a number of system components, including the UAS bare airframe flight dynamics, airwake, and the motion of the ship deck. These elements are merged into a single simulation environment using multi-body dynamics modelling in FLIGHTLAB® (Ref. 23). In addition, software-in-the-loop (SITL) and hardware in-the-loop (HITL) simulations are performed using dedicated equipment.

3.1. Bare airframe dynamics

Figure 3 shows a graphical view of the EVO VTOL UAS research vehicle. Computational Fluid Dynamics (CFD) simulations have been performed using NLR's in-house ENSOLV software to establish an aerodynamic database of the lifting surface, elevons, and propeller elements. In combination with the scanned geometry, vehicle mass and inertia, and (assumed) actuator dynamics, a FLIGHTLAB®

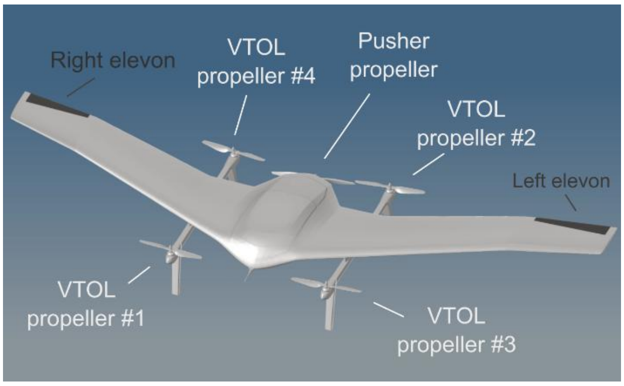

Figure 3: DeltaQuad EVO platform layout

model of the EVO is created. FLIGHTLAB® is a component-based simulation environment that allows the designer to choose aerodynamic and structural models of different fidelity for individual components to capture relevant physics while still providing (near) real-time capability for dynamic simulations. This makes it particularly suitable for efficient modelling of novel configurations that involve aero-propulsive interactions. For initial modeling of the EVO rotor forces and moments, blade element models serve as the chosen formulation, whereas a Peters-He inflow model (Ref. 24) is used for rotor-wing interference. Blade dynamics and aeroservoelasticity are not included as these effects are not expected to be significant on the demonstrator platform in the airspeeds considered. As the project progresses, the bare airframe model will be further improved and validated against flight test data.

3.2. Control law interface

A functional mock-up (FMU) interface between FLIGHTLAB® and Simulink® enables the implementation and valuation of flight control laws as part of dynamic simulations of the closed-loop system. The use of FMUs also simplifies the use of other MATLAB® software tools used during development, such as CONDUIT® (Ref. 25). Moreover, the developed control laws can be integrated into SITL/HITL simulations thanks to the MATLAB® UAV Toolbox Support Package for PX4 Autopilots (Ref. 26). This package enables rapid deployment and testing of a controller on an experimental PX4 flight control computer. Combined, these tools enable rapid and effective prototyping and task-oriented testing of different control law configurations.

3.3. Ship deck environment

The distinctive characteristics of ship deck operating environments require a multidisciplinary modelling approach. This aims at two central aspects: i) the interaction between the UAS and the air wake induced by the superstructure of the ship when operating in different relative wind conditions; and ii) the motion of the ship deck in different sea states and wave directions. Ship motion data is obtained from XMF (eXtensible Modeling Framework) computations performed by the Maritime Research Institute Netherlands (MARIN). Together with CFD ship air wake data obtained from the MARIN software tool ReFRESCO, these datasets allows to run closed-loop simulations for a variety of scenarios. More details about the ship deck simulation environment can be found in Ref. 4.

Figure 4: Experimental motion base platform

In addition to the FLIGHTLAB® model setup, ship deck motion will also be simulated using a physical motion base platform as part of a fully integrated system validation exercise (see Figure 4). This enables flight tests of the EVO demonstrator on a landing platform that simulates the heave, roll and pitch motion expected on a ship deck environment in adverse conditions.

4. LANDING TRAJECTORY PLANNING

The ship-UAS guidance logic represents a key technology enabler and has been subject of previous research by the project partners (see Ref. 4). For the landing trajectory, a strategy is selected that combines a relative position hold controller in the horizontal direction with a pre-planned vertical velocity profile and -controller. First, the VTOL UAS will fly towards a point above the ship deck. Next, the position hold mode is engaged to hold the position relative to the ship deck. In the third phase, the landing is initiated. This final phase is executed through an exponential (relative) height profile (Ref. 1):

$$h = (h - h_{deck})|_{t=0} e^{-t/\tau} + h_{deck} \quad (1)$$

where h_0 is the height above the deck at which the landing maneuver is initiated, τ is a constant and t is the time elapsed since the start of the maneuver. Differentiation of the exponential law provides the height rate control signal which is proportional to the height above the deck. A constant term is added to this equation to anticipate for ship heave velocity:

$$\dot{h}_{ref} = -\frac{1}{\tau}(h - h_{deck}) + \dot{h}_{deck} \quad (2)$$

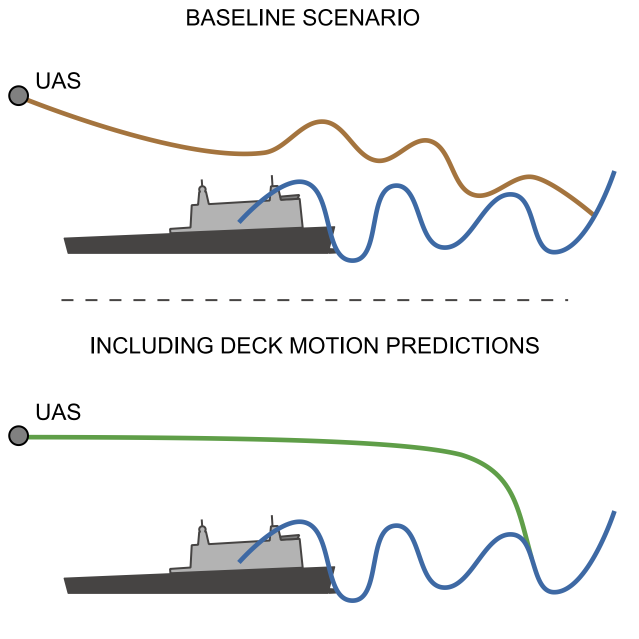

Figure 5: Comparison of two landing algorithms highlighting the value of using predictions of future deck motion (illustration based on Refs. 3,4,17)

In Ref. 4, this strategy was presented as a baseline scenario. Subsequently, the automated landing with pre-planned velocity profile is to be extended with touch-down timing. This can be done by initiating the landing based on the energy level of the ship's motion, as introduced in Ref. 2, or through real-time planning and updating of the velocity profile based on motion prediction. A combination of these methods is also possible. Real-time use of deck motion predictions avoids vertical oscillations due to the tracking relative to the ships motion by following a direct path to the final landing state, as depicted in Figure 5. In previous work by one of the authors (Ref. 4), the landing point is chosen in the middle of a time interval in which the ship deck has a fairly constant downward motion for a relatively long duration. An analysis of the ship air wake can help to further optimize a 4D landing trajectory in space.

In order to predict the ship motion, sensors will be installed on a ship deck and a prediction model using either autoregressive moving averages (ARMA) or adaptive notch filters (ANF) employed (Ref. 27). These methods result in relatively consistent and effective model parameter adaptation when conditions are changing, while being fairly easy to implement. The motion prediction will be sent to the UAS through a datalink for onboard trajectory planning.

5. CONTROL LAW DESIGN FRAMEWORK

To ensure adequate flying characteristics as the lift-and-cruise UAS moves closer to its operating limits, robust, high-performance flight control laws are required. Therefore, a well-defined set of design objectives and constraints should be determined for the mission at hand. These requirements should translate to the control design in a clear and verifiable manner. The robust control framework provides important instruments to achieve translation in a systematic and theoretically sound fashion.

5.1. Design requirements

When flying in strong winds and in the air wake of a ship's superstructure, good gust and turbulence rejection properties are crucial for precise trajectory following and safe landing. Disturbance rejection therefore represents a key design goal. However, the controller bandwidth must strike a balance, being wide enough to capture and reject disturbances while maintaining stability and robustness. This relates to several aspects, including the avoidance of excessive use of control authority, actuator overdriving, and structural mode excitation. Since many of these aspects are effectively dictated by the available hardware itself, there is a clear limitation on the total bandwidth available for disturbance rejection purposes. Therefore, it is of importance to get insight into the frequency spectrum where attenuation is needed for the mission at hand.

Since recent years, active research has been done into disturbance rejection criteria in terms of the disturbance rejection bandwidth (DRB) and disturbance rejection peak (DRP) for manned rotorcraft

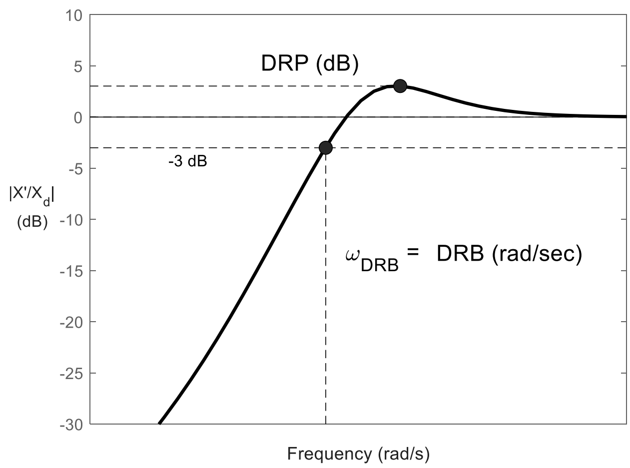

Figure 6: Disturbance Rejection Bandwidth (DRB) and Peak (DRP) definitions (based on Ref. 28)

Table 1: Example overview of selected design objectives (note: list is non-exhaustive)

Category	Example criteria	Evaluation
Disturbance rejection	DRB, DRP, CETI response, SUOLs	Freq.-domain analysis, $\mathcal{H}_\infty$-norms, non-linear simulations, Monte Carlo, etc.
Flying qualities	Damping, quickness, closed-loop bandwidth/phase delay, LOES parameters	
Robustness	Stability margins, crossover freq., airframe parameter sensitivity	
Control margin	Actuator activity, saturation rate	

(Ref. 28). These criteria are defined as shown in Figure 6 and are reported to be incorporated into the future ADS-33F-PRF standard. They provide an indication of how sensitivity functions should be shaped in magnitude. However, the corresponding performance boundaries will need to be modified to be suitable for small-scale unmanned operation. A useful instrument here is Froude scaling, as proposed by Ivler *et al*. in Ref. 29.

As an alternative to these guidelines, explicit disturbance modeling can be performed. The approach described in Ref. 11 can be adopted to model the vehicle response to turbulence with a control equivalent turbulence input (CETI) representation, which drives the controls of the aircraft to reproduce realistic motion caused by turbulence and corresponding power spectra as demonstrated for different UAV configurations in Refs. 9 and 10. This is used to identify the frequency range at which the feedback control response should provide attenuation. Similar to Refs. 9 and 10, a control requirement is defined to minimize the RMS (3σ) of the error signal in the frequency domain due to CETI turbulence, amounting to minimizing the 3σ deviation of the aircraft response from trim due to CETI turbulence.

A second category of requirements considers the flying characteristics of the UAS in a broader sense. This aspect concerns both automatic path-following as well as (optional) manual handling. For lift-and-cruise UAS, the desired dynamics can be categorized according to the three main modes of operations: hover, transition, and forward flight. Accordingly, different response type characteristics may need to be selected for each of these modes. To achieve the desired response properties, specific handling criteria as listed in airworthiness standards (e.g., ADS-33, see Ref. 30) for large-scale manned vehicles can be used. Typical handling quality requirements include a minimum closed-loop bandwidth, damping, quickness (related to available control authority) and coupling between individual axes. However, target values should again be transformed to be applicable to small-scale UAS.

Finally, in line with the previous discussion, specific attention is given to robustness, control activity, and saturation handling. Robustness relates to classical and multi-channel stability margins at both the airframe input and sensor outputs, with extensions to parametric uncertainty. Control activity is to be minimized to limit actuator degradation and to maximize authority. Although the latter ensures that saturation is postponed, it can be expected that flying in strong winds will lead to frequent saturation of one or multiple effectors. Under these circumstances, the controller shall remain stable and ensure a gradual degradation of performance.

5.2. Robust control framework

The multi-objective set of design requirements (see Table 1) represents a combination of high- and low-level objectives and constraints that should be translated to a systematic control design strategy. The robust control framework is fundamental to systematic analysis and design of controllers that need to comply with precise performance goals in the face of uncertainty. Figure 7 shows the typical system interconnection that illustrates how a controller K interacts through inputs u and observations y with a generalized plant P that is affected by external dis-

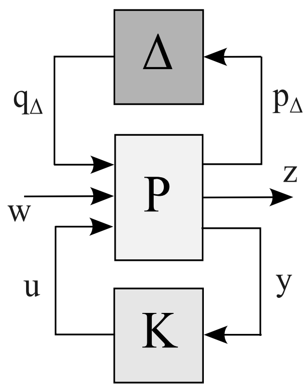

Figure 7: Generalized system interconnection

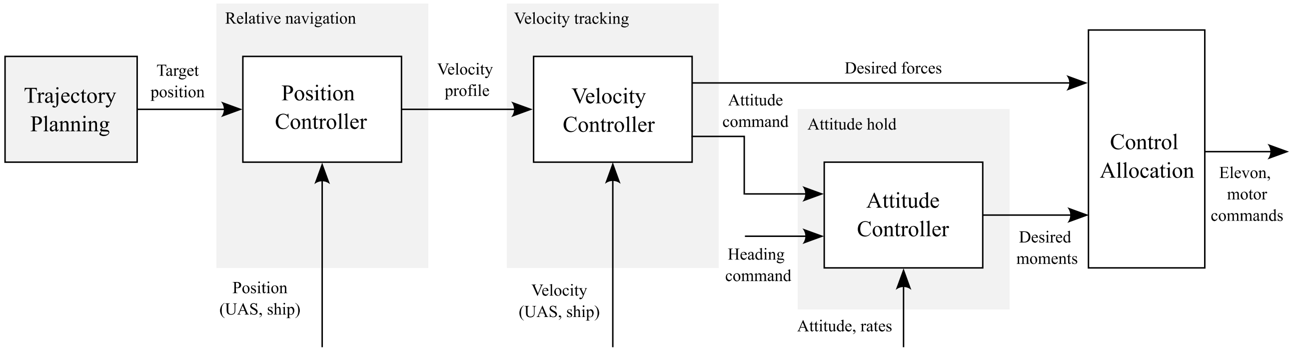

Figure 8: High-level unified INDI control law; the benchmark PID setup is similarly configured in hover mode

turbance signals w and some form of uncertainty Δ. Observations of the resulting closed-loop system dynamics are obtained through z. Then, the design objective can generally be stated as the minimization of the worst-case $\mathcal{H}_\infty$-norm:

$$\min_{\mathrm{K}\in\mathrm{K}} \max_{\Delta\in\mathbf{\Delta}} \|\mathrm{W_L}\mathcal{F}_\ell(\mathcal{F}_u(\Delta, P), K)\mathrm{W_R}\|_\infty < \gamma \qquad (1)$$

For more detailed background, the reader is referred to, e.g., Refs. 31, 32. Depending on the problem definition, a variety of different methods and implementations exist. For example, in the classical case of full-order $\mathcal{H}_\infty$-synthesis, the controller structure is left unspecified and nominal loop-shaping considerations are used to maximize robustness against implicit forms of full-block dynamic uncertainty. Another case is to optimize specific parameters of some *a-priori* specified structured control law against an explicit combination of dynamic and parametric uncertainty, which can be referred to as structured mixed μ-synthesis. Whereas these methods are commonly presented for Linear Time-Invariant (LTI) systems, extensions to Linear Parameter-Varying (LPV) systems also exist (see, e.g., Ref. 33).

What these methods share as a common basis is that the optimal controller is directly determined by the problem definition itself; i.e., in other words, it is the product of the combination of the (nominal) plant behavior, the anticipated level of uncertainty, and the performance requirements (disturbance rejection, tracking behavior, etc.) as specified by the designer. This makes the robust control framework a natural choice in light of the multi-objective set of design requirements specified before.

Since the fundamental trade-offs and implications captured by $\mathcal{H}_\infty$-machinery are of vital importance to sound robust design, it serves as the central framework for parameter synthesis for the candidate control law structures in the project. However, an important consideration is that not all design criteria can be easily translated to norm-based objectives (e.g., $\mathcal{H}_\infty$ or $\mathcal{H}_2$). This applies in particular to some nonlinear time-domain requirements. To this end, the 'control-theoretic' robust framework is combined with the 'process-oriented' design approach used in CONDUIT® (Ref. 25). This implies that a translation to norm-based descriptions is made where possible, while additional time-domain evaluations are performed for specific criteria. This strategy is also reflected in Table 1, which lists a combination of different evaluation methods for the presented criteria.

6. CONTROL LAW ARCHITECTURES

Two different control law architectures are investigated in the project, with an overview provided in the following section. The first option represents a benchmark design based on a classical, cascaded PID structure with mode-blending, whereas the second setup corresponds to a unified control approach based on the principle of Incremental Nonlinear Dynamic Inversion (INDI). A high-level illustration of the unified INDI control law architecture, including the common elements shared by the benchmark PID controller, is provided in Figure 8. Here, the different modes of operation can be recognized from the multi-loop configuration. This setup allows for the selection of different (manual) flight modes. For relative position and velocity control during the automated landing, a DGPS sensor solution will be used that provides a relative position error to the UAS.

6.1. Blending cascaded PID benchmark

The first architecture consists of a combination of classical, cascaded PID controllers that are blended as the UAS changes flight mode (i.e., from hover to wing-borne flight and vice versa). The corresponding logic ensures that the appropriate effectors are used as the UAS traverses the transition corridor. This architecture is equivalent to the PX4 stock controller. In fixed-wing flight mode, the PX4 position controller consists of additional logic based on the Total Energy Control System (TECS; initially proposed in Ref. 34) and nonlinear path-following guidance (see, e.g., Refs. 35 and 36) concepts. With the former, throttle and pitch attitude commands are generated by energy balance computations. Additionally, turn coordination logic is incorporated to minimize lateral acceleration.

The PID control gains serve as the primary design parameters to optimize the control law according to the design requirements listed before (stable eigenvalues, bandwidth, stability margins, etc.). However, due to the fact that the overall architecture is left unmodified, the overall performance gain is expected to be limited. Since operations on a naval ship deck will likely include significant spatial and temporal differences in turbulence intensity, it is anticipated that the UAS will operate in the transition corridor for significant amounts of time. This creates the possibility for irregular switching between flight modes and may lead to inadequate use of the available control authority. Therefore, a second, incremental control law, configured for unified operation over the flight envelope, is designed in parallel.

6.2. Unified INDI control law

The INDI principle is applied to resolve both the translational and rotational dynamics of the VTOL UAS (i.e., rates and accelerations). With this approach, the aim is to transform the nonlinear airframe dynamics to a desired form. The proposed setup integrates the corresponding INDI loops into a unified control structure that maps desired trajectories through an intermediate kinematic transformation onto direct propulsion forces and vehicle attitude. Consequently, attitude is treated as a virtual control variable that is to be resolved through an intermediate kinematic mapping to desired effector moments. This approach is known as the time-scale separation principle and is illustrated in Figure 8. Examples in the literature of similar setups applied to VTOL vehicles can be found in Refs. 18-22.

6.2.1. Background

Incremental Nonlinear Dynamic Inversion (INDI) is a control strategy that gained popularity in recent years and that simplifies the inversion of a nonlinear system through Taylor-series linearization. (Ref. 14) Acceleration measurements allow to find the required actuator increment from the acceleration error through inversion of the control effectiveness. The resulting, simplified control law reads as follows:

$$\Delta u_c = B^{-1}(\nu - \dot{y}_0) \quad (3)$$

$$u_c = u_0 + \Delta u_c \quad (4)$$

where B represents the (local) control effectiveness matrix, u the actuator command vector, $\nu = \dot{y}_c$ the pseudo-control vector and the subscript ‘0’ refers to the previous time-step. Thanks to the incremental form, the plant dynamics do not need to be in affine form with the control input. Applied to aircraft rate control, a sensor-based approach to INDI effectively treats the system dynamics as a disturbance that is measured through acceleration feedback ($\dot{y}_0$) and compensated for by fast actuator action. The key concept of this approach, therefore, lies in its ability to compute control inputs based on acceleration measurements and local actuator effectiveness, rather than relying on a full dynamic model. Consequently, with respect to automated UAV landings on naval ship decks, sensor-based INDI reduces dependency on an accurate aerodynamic model (e.g. in the presence of ground effect and other aerodynamic interactions with the ship’s superstructure). Moreover, it provides effective rejection of external disturbances, as demonstrated in Ref. 15 for a quadcopter and in Ref. 16 for a tail-sitter.

6.2.2. Robustness considerations

Despite its seemingly attractive benefits, the use of sensor-based INDI must be carefully considered in light of overall robustness. This is due to the fact that this type of controller effectively generates high-gain, high-bandwidth feedback control action, as discussed in Ref. 37. To this end, it is common practice to adopt carefully tuned feedback filters to avoid actuator wear and excitation of structural modes from acceleration feedback signals:

$$\Delta u_c = B^{-1}\left(\nu - \hat{\dot{y}}_0\right), \qquad \hat{\dot{y}}_0 = H_c \dot{y}_0 \quad (5)$$

$$u_c = \hat{u}_0 + \Delta u_c, \qquad \hat{u}_0 = H_{sync} u_0 \quad (6)$$

Here, H_c serves as an (equivalent) compensation filter (typically a low-pass filter). The filter H_{sync} is used to ‘synchronize’ the input feedback signal with the filtered acceleration signal (Ref. 38). Alternatively, a combination of model-based and sensor-based inversion can also be used. For example, a scaled complementary filter (SCF) as proposed in Ref. 39. can be used to blend both prediction signals as a function of frequency:

$$\begin{aligned}\hat{\dot{y}}_0 &= (1 - K_c H_c)\dot{y}_0^{(MB)} + K_c H_c \dot{y}_0 \\ &= \dot{y}_0^{(MB)} + K_c H_c e_{y_0}\end{aligned} \quad (7)$$

Here, $K_c \in [0,1]$ represents the compensation gain, whereas H_c is referred to as the compensation filter in this context. Setting $K_c = 1$ and disconnecting the model prediction signal make the inversion strategy collapse to the filtered sensor-based variant from above. Tuning these inversion compensation parameters allows the designer to set the bandwidth associated with the inversion loop and thereby balance out disturbance rejection performance with the robustness properties mentioned before. Together with the virtual control parameters associated with the pseudo-control input ν and the selected representation of the on-board model, they represent the main design parameters to satisfy the design requirements. As shown in Refs. 37 and 39, this can be done systematically using the $\mathcal{H}_\infty$-framework.

6.2.3. Control allocation

The control allocation module is of central significance to the unified control design strategy. Here, a condition-dependent effector weighting scheme enables a smooth transition of priorities over the flight envelope. For example, the gradual conversion from propeller-induced attitude changes in hover mode to the use of control surfaces in forward-flight can be achieved by allocating the available effectors as a function of airspeed. A popular and effective method that is implementable in closed form while having bounded run-time at the same time is the weighted pseudo-inverse (Refs. 40, 41), which takes the form:

$$K_{alloc}(.) = W(.)^{-1} B^T (B W(.)^{-1} B^T)^{-1} \quad (8)$$

Here, $W(.)$ represents a weighting matrix as selected by the designer and B is the (local) control effectiveness matrix from before. The unified control structure allows the control law to remain the same throughout the entire flight envelope, while the control allocation provides a smooth transition in effector use according to their effectiveness between hover and fixed-wing flight. This is particularly beneficial for landing on a ship in adverse weather. When keeping its relative position over the deck of a sailing naval vessel in relative winds, the UAS will regularly operate in a velocity regime similar to transition for prolonged times. Instead of continuously switching between distinct controllers for hover and fixed-wing flight, the proposed controller should allow for efficient trim and control in this intermediate regime. Using the attitude commands as virtual controls in a combined allocation allows to maximize vertical control authority for gust rejection and for accurate vertical velocity tracking during landing, but comes with a number of challenges.

Effector saturation requires dedicated solutions in the control design. In the case sufficient control authority is available to meet the acceleration demands (i.e., in the “over-actuated” or “exactly actuated” case), control allocation shall aim for an effector distribution that maximizes the distance to the respective saturation limits. This can be achieved by finding control solutions for which the ℓ_2-norm between the actual and desired (typically zero) effector quantity (e.g., position, RPM) is minimized within the null-space of the control effectiveness matrix. Such an additional step in the null-space towards a “preferred solution” also serves to resolve the path-dependency problem of incremental control allocation that can otherwise lead to undesired configurations and early effector saturation (Refs. 40,42,43). Popular approaches to solve the constrained allocation problem, which arises from effector rate and position limits, are cascaded (iterative) pseudo-inverse approaches or linear and quadratic programming (Ref. 41). In both cases, the error weighting matrix can be used to prioritize control around individual axes. In case the demands cannot be met (i.e., the “underactuated” scenario), axis prioritization and anti-windup will need to be performed. Here, a strategy must be determined which control variables are prioritized. Heave and pitch are typically given precedence to over roll and yaw, to ensure that a safe vertical flight path is maintained.

6.2.4. Anti-windup compensation

Anti-windup compensation ensures that saturation does not result in a controller-induced loss of stability and performance for the underactuated scenario. In the case of integral action, this technique prevents the integrator state from accumulating tracking errors that will need to ‘wind down’ over time once the system returns to an unconstrained condition. This same principle also applies to general multivariable controllers with many states (Ref. 44). Accordingly, design of anti-windup compensators can be performed based on a formal framework that ensures stability and desired input-output behavior according to some performance norm. As outlined in Ref. 44, the two main approaches to the design of modern anti-windup algorithms can be categorized as *direct linear anti-windup* (DLAW) and *model recovery anti-windup* (MRAW). Similar to 'unconstrained' controllers, these compensators can be of dynamic or static nature. The concept of *pseudo-control hedging* (PCH), popular in the context of (I)NDI control architectures (see Refs. 45, 46), can be viewed as a special example of an MRAW scheme of the latter type.

6.3. Flight envelope protection

To prevent the UAS from entering flight conditions that will be difficult or impossible to recover from (e.g., all authority is lost), additional schemes will need to be established. This applies in particular to scenarios that involve aerodynamic wing stall or excessive levels of sideslip. Irrespective of the control law (PID or INDI), the initial strategy during hover will include controlling sideslip to zero (weather vaning) and limit pitch and roll angle commands to reduce susceptibility to gusts. Here, it should be remarked that during hover with respect to a moving ship deck, the (relative) airspeed may be significant. This will result in nonzero sideslip, which is fundamentally different from a pure (i.e., stationary) hover scenario. During the project, the precise effects of sideslip in combination with strong winds on landing performance will be investigated in detail.

7. CONCLUDING REMARKS

The project is currently in its design phase, during which a number of technical challenges are being addressed that are specific to the application at hand but that are also of wider relevance. A specific example is the topic of stability and performance implications resulting from a mix of physical and virtual control effectors of varying bandwidth in a multi-loop control allocation setup. This is an area of significant interest that standard INDI and feedback linearization theory do not consider. Another example is the systematic design of anti-windup algorithms in combination with incremental controllers.

Fully integrated nonlinear simulations and land-based flight tests are planned in the upcoming months. Ultimately, the proposed control approach is to be validated by means of flight testing at sea on the LPD-2 naval ship deck.

Author contact:

Tijmen Pollack tijmen.pollack@nlr.nl

Ole Pfeifle ole.pfeifle@nlr.nl

Stefan van 't Hoff stefan.van.t.hoff@nlr.nl

George T. Alevras george.tzanetos.alevras@nlr.nl

Jan-Willem van Doorn jan-willem.van.doorn@nlr.nl

Mark Voskuijl m.voskuijl@mindef.nl

Eelco Frickel e.frickel@marin.nl

8. ACKNOWLEDGMENTS

This work is carried out as part of the Defense technology project N23/013 ShiP-deck Environment and Efficient Drone OPerationS (SPEEDOPS) funded by the Dutch Ministry of Defense.

9. REFERENCES

1. Blakelock, J., *Automatic Control of Aircraft and Missiles,* John Wiley & Sons, New York, NY, 1991, Chapter 2.
2. Ferrier, B., and Manning, T., "Simulation and testing of the landing period designator (LPD) helicopter recovery aid," *Naval Engineers Journal*, Vol. 110, (1), 1998, pp. 189-205. DOI: 10.1111/j.1559-3584.1998.tb02396.x.
3. Hendrick, C., and Horn, J., "Analysis of flight control and trajectory planning for autonomous ship landing using small-scale UAVs," Proceedings of the 48th European Rotorcraft Forum, Winterhur, Switzerland, 2022.
4. Voskuijl, M., Bakker, R., Zilver, D., and van Rooij, M., "Autonomous ship deck landing strategies for unmanned rotorcraft operating in harsh weather conditions," The Vertical Flight Society's 81st Annual Forum and Display, Virginia Beach, VG, 2025.
5. Hoencamp, A., *Helicopter-Ship Qualification Testing The Theory and Application of a Novel Test Methodology Optimizing for Cost and Time Efficiency*, Delft, The Netherlands: PhD thesis, Delft University of Technology, 2015.
6. Zilver, D., Varriale, C., and Voskuijl, M., "Optimal UAV Approaches in Wind-Affected Maritime Operations Trajectory optimization of an unmanned helicopter to a ship's deck in various wind conditions," The Vertical Flight Society's 81st Annual Forum and Display, Virginia Beach, VG, 2025.
7. Cademartori, G., Oneto, L., Valdenazzi, F., Coraddu, A., Gambino, A., and Anguita, D., "A review on ship motions and quiescent periods prediction models," *Ocean Engineering*, Vol.

280, 2023, 114822. DOI: 10.1016/j.oceaneng.2023.114822.

8. Triantafyllou, M., Bodson, M., and Athans, M., “Real time estimation of ship motions using Kalman filtering techniques,” *IEEE Journal of Oceanic Engineering*, Vol. 8, (1), 1983, pp. 9-20. DOI: 10.1109/JOE.1983.1145542
9. Berrios, M., Berger, T., Tischler, M., Juhasz O., and Sanders, F., “Hover Flight Control Design for UAS Using Performance-based Disturbance Rejection Requirements,” American Helicopter Society 73rd Annual Forum, Fort Worth, TX, 2017.
10. Juhasz, O., Tischler, M., and Won, H., “System Identification and Control Law Optimization Applied to the AeroVironment Quantix Tail-Sitter UAS,” American Helicopter Society 74th Annual Forum, Phoenix, AZ, 2018.
11. Juhasz, O., Lopez, M., Berrios, M., Berger, T., and Tischler, M., “Turbulence Modeling of a Small Quadrotor UAS Using System Identification from Flight Data,” American Helicopter Society 73rd Annual Forum, Fort Worth, TX, 2017.
12. Fernandez, R., Dominguez, S., and Campoy, P., “L1 Adaptive Control for Wind Gust Rejection in Quad-Rotor UAV Wind Turbine Inspection,” International Conference on Unmanned Aircraft Systems, Miami, FL, 2017.
13. Cui, L., Zhang, R., Zang, H., and Zuo, Z., “Adaptive super-twisting trajectory tracking control for an unmanned aerial vehicle under gust winds,” Aerospace Science and Technology, Vol. 115, 2021, pp. 106833. DOI: 10.1016/j.ast.2021.106833
14. Sieberling, S., Chu, Q., and Mulder, J., “Robust Flight Control Using Incremental Nonlinear Dynamic Inversion and Angular Acceleration Prediction,” Journal of Guidance, Control, and Dynamics, Vol. 33, (6), 2010, pp. 1732-1742. DOI: 10.2514/1.49978
15. Smeur, E., de Croon, G., and Chu, Q., “Cascaded incremental nonlinear dynamic inversion for MAV disturbance rejection,” Control Engineering Practice, Vol. 73, 2018, pp. 79-90. DOI: 10.1016/j.conengprac.2018.01.003
16. Smeur, E., Bronz M., and de Croon, G., “Incremental Control and Guidance of Hybrid Aircraft Applied to a Tailsitter Unmanned Air Vehicle”, Journal of Guidance, Control, and Dynamics, Vol. 43, (2), 2020, pp. 274-287. DOI: 10.2514/1.G004520
17. Hendrick, C., Nicholson, D., Jaques, E., Horn, J., Langelaan J., and Sydney, A., "Scaled Experiments in Flight Control Design for Autonomous Landing in High Sea States," Paper AIAA 2022-3280, AIAA AVIATION 2022 Forum, Chicago, IL & Virtual , 2022. DOI: 10.2514/6.2022-3280.
18. Raab, S., Zhang, J., Bhardwaj, P., and Holzapfel, F., "Proposal of a Unified Control Strategy for Vertical Take-off and Landing Transition Aircraft Configurations," Paper AIAA 2018-3478, 2018 Applied Aerodynamics Conference, Atlanta, GA, 2018. DOI: 10.2514/6.2018-3478.
19. Lombaerts, T., Kaneshige, J., Schuet, S., Aponso, B., Shish, K., and Hardy, G., "Dynamic Inversion based Full Envelope Flight Control for an eVTOL Vehicle using a Unified Framework," Paper AIAA 2020-1619, AIAA Scitech 2020 Forum, Orlando, FL, 2020. DOI: 10.2514/6.2020-1619.
20. Milz, D., and Looye, G., "Tilt-Wing Control Design for a Unified Control Concept," Paper AIAA 2022-1084, AIAA SCITECH 2022 Forum, San Diego, CA & Virtual, 2022. DOI: 10.2514/6.2022-1084
21. Saetti, U., “Dynamic Inversion Flight Control Laws for Automatic Transition of Tilt-Rotor/Wing Aircraft,” *Journal of the American Helicopter Society*, Vol. 70, (3), 2025, pp. 1-21. DOI: 10.4050/JAHS.70.032005
22. De Wagter, C., Remes, B., Smeur, E., Van Tienen, F., Ruijsink, R., Van Hecke, K., and Van der Horst, E., “The NederDrone: A hybrid lift, hybrid energy hydrogen UAV”, *International Journal of Hydrogen Energy*, Vol. 46, (29), 2021, pp. 16003-16018. DOI: 10.1016/j.ijhydene.2021.02.053.
23. Du Val, R., and He, C., “Validation of the FLIGHTLAB virtual engineering toolset,” *The Aeronautical Journal*, Vol. 122, (1250), pp. 519-555, 2018. DOI: 10.1017/aer.2018.12.
24. Peters, D., and He, C., “Finite State Induced Flow Models Part II: Three-Dimensional Rotor Disk,” *Journal of Aircraft*, Vol. 32, (3), 1995, pp. 323-333. DOI: 10.2514/3.46719.
25. Tischler, M., Berger, T., Ivler, C., Mansur, M., Cheung, K., and Soong, J., *Practical Methods for Aircraft and Rotorcraft Flight Control Design: An Optimization-Based Approach*, American Institute of Aeronautics and Astronautics, Reston, VA, 2017, Chapter 3.
26. The MathWorks Inc., “UAV Toolbox Support Package for PX4 Autopilots (R2025a)”, Natick, Massachusetts: The MathWorks Inc., 2025. https://www.mathworks.com/help/uav/px4-spkg.html (Retrieved July 25, 2025).
27. Monneau, A., M’Sirdi, N., Mavromatis, S., Varra, G., Salesse, M., and Sequeira, J., “Adaptive Prediction for Ship Motion in Rotorcraft Maritime Operations“, *CEAS Aeronautical Journal*,

Vol. 11, 2020, pp. 1071-1082. DOI: 10.1007/s13272-020-00470-x.

28. Berger, T., Ivler, C., Berrios, M., Tischler, M., and Miller, D., “Disturbance Rejection Handling Qualities Criteria for Rotorcraft,” American Helicopter Society 72nd Annual Forum, West Palm Beach, FL, 2016.
29. Ivler, C., Truong, K., Kerwin, D., Otomize, J., Parmer, D., Tischler, M., and Gowans, N., “Development and Flight Validation of Proposed Unmanned Aerial System Handling Qualities Requirements,” *Journal of the American Helicopter Society*, vol. 67, (1), 2022, pp. 1-18. DOI: 10.4050/JAHS.67.012002.
30. Anonymous, “Aeronautical Design Standard, Performance Specification: Handling Qualities Requirements for Military Rotorcraft,” ADS-33, U.S. Army Aviation Systems Command, 1987.
31. Skogestad, S., and Postlethwaite, I., *Multivariable Feedback Control: Analysis and Design*, John Wiley & Sons, Chichester, United Kingdom, 2005.
32. Apkarian, P., and Noll, D., “The $\mathcal{H}_\infty$ Control Problem is Solved,” *Aerospace Lab*, Vol. 13, 2017, p. 1-11. DOI: 10.12762/2017.AL13-01.
33. Rugh, W., and Shamma, J., “Research on gain scheduling”, *Automatica*, Vol. 36, (10), 2000, pp. 1401-1425. DOI: 10.1016/S0005-1098(00)00058-3.
34. Lambregts, A., "Vertical flight path and speed control autopilot design using total energy principles," Paper AIAA 1983-2239, Guidance and Control Conference, Gatlinburg, TN, 1983. DOI: 10.2514/6.1983-2239.
35. Park, S., Deyst, J., and How, J., “Performance and Lyapunov Stability of a Nonlinear Path Following Guidance Method,” Journal of Guidance, Control, and Dynamics, vol. 30, (6), 2007, pp. 1718–1728. DOI: 10.2514/1.28957.
36. Stastny, T., and Siegwart, R., "On Flying Backwards: Preventing Run-away of Small, Low-speed, Fixed-wing UAVs in Strong Winds," 2019 IEEE/RSJ International Conference on Intelligent Robots and Systems (IROS), Macau, China, 2019, pp. 5198-5205, DOI: 10.1109/IROS40897.2019.8968573.
37. Pollack, T., and Van Kampen, E., “Robust Stability and Performance Analysis of Incremental Dynamic-Inversion-Based Flight Control Laws” Journal of Guidance, Control, and Dynamics, 46, (9), 2023, pp. 1785-1798. DOI: 10.2514/1.G006576.
38. Grondman, F., Looye, G., Kuchar, R., Chu, Q., and Van Kampen, E., "Design and Flight Testing of Incremental Nonlinear Dynamic Inversion-based Control Laws for a Passenger Aircraft," Paper AIAA 2018-0385, 2018 AIAA Guidance, Navigation, and Control Conference, Kissimmee, FL, 2018. DOI: 10.2514/6.2018-0385.
39. Pollack, T., Theodoulis S., and Van Kampen, E., “Commonalities between robust hybrid incremental nonlinear dynamic inversion and proportional-integral-derivative flight control law design”, *Aerospace Science and Technology*, 152, 2024, pp. 109377. DOI: 10.1016/j.ast.2024.109377.
40. Durham, W., Bordignon, K., and Beck, R., “*Aircraft Control Allocation*”, John Wiley & Sons, Chichester, United Kingdom, 2017.
41. Johansen, T., and Fossen, T., “Control allocation—A survey”, *Automatica*, Vol. 49, (5), 2013, pp. 1087-1103. DOI: 10.1016/j.automatica.2013.01.035.
42. Pfeifle, O., and Fichter, W., “Minimum Power Control Allocation for Incremental Control of Over-Actuated Transition Aircraft”. Journal of Guidance, Control, and Dynamics 46(2), 286-300, 2023. DOI: 10.2514/1.G006929.
43. Pollack, T., and Van Kampen. E., "Multi-objective Design and Performance Analysis of Incremental Control Allocation-based Flight Control Laws," Paper AIAA 2023-1249, AIAA SCITECH 2023 Forum, National Harbor, MD & Online, 2023. DOI: 10.2514/6.2023-1249.
44. Galeani, S., Tarbouriech, S., Turner, M., and Zaccarian, L., “A Tutorial on Modern Anti-windup Design”, *European Journal of Control* 15, (3-4), 418-440, 2009. DOI: 10.3166/ejc.15.418-440.
45. Holzapfel, F., and Sachs, G., "Dynamic Inversion Based Control Concept with Application to an Unmanned Aerial Vehicle," Paper AIAA 2004-4907. AIAA Guidance, Navigation, and Control Conference and Exhibit. Providence, RI, 2004. DOI: 10.2514/6.2004-4907.
46. Lombaerts, T., and Looye, G.,. "Design and flight testing of manual nonlinear flight control laws," Paper AIAA 2011-6469, AIAA Guidance, Navigation, and Control Conference, Portland, OR, 2011. DOI: 10.2514/6.2011-6469.